Physics Letters B 664 (2008) 70–77

Contents lists available at ScienceDirect

Physics Letters B

www.elsevier.com/locate/physletb

Single pion production in CC $\nu_\mu N$ scattering within a consistent effective Born approximation

C. Barbero [a], G. López Castro [b,1], A. Mariano [a,*]

[a] Departamento de Física, Facultad de Ciencias Exactas, Universidad Nacional de La Plata, cc. 67, 1900 La Plata, Argentina
[b] Instituto de Física, Universidad Nacional Autónoma de México, México D.F., C.P. 04510, Mexico

ARTICLE INFO

Article history:
Received 18 February 2008
Received in revised form 15 April 2008
Accepted 1 May 2008
Available online 9 May 2008
Editor: G.F. Giudice

PACS:
25.30.Pt
25.75.Dw
14.20.Gk

ABSTRACT

The one pion production in charged current $\nu_\mu N$ scattering is analyzed within an extended version of a model used previously to include the $\Delta(1232)$ contribution in elastic and radiative pion–nucleon scattering, and in pion photoproduction. Because the resonant amplitude needs to be invariant under contact transformations, we identify the correct forms of the Δ propagator and the $W^- N\Delta$ vertex that are consistent with this requirement. The only free parameter of the model, the axial form factor at zero momentum transfer, is fixed from data on the differential cross section for $\nu_\mu p \to \mu^- p\pi^+$ scattering. A reasonable agreement with the experimental data of all the $\nu N \to \mu N'\pi$ total cross sections is obtained. We show that the use of the complete Δ propagator instead of the Rarita–Schwinger one improves the theoretical results, leading to differences ranging from 10 to 30%, depending on the specific process.

The interest on weak pion production processes from νN collisions is twofold: (i) they have become a very important element in the analysis of neutrino oscillation experiments, and (ii) they are a powerful tool to study the hadron structure. For example, in the atmospheric neutrino experiment at Kamioka [1], the energy spectrum of weak pion production amounts a 20% of the quasielastic lepton production cross section and it is the major source of uncertainty in the identification of electron and muon events. In addition, neutral current π^0 production might play an important role to distinguish between different oscillation mechanisms of neutrinos produced at accelerators [2–4]. Thus, it is important to have under good control all possible contributions to the $\nu N \to lN'\pi$ cross section. In particular, it is important to have another check of the hadronic matrix element of these processes, which involves the contribution of nucleonic resonances. This is usually done by using effective dynamical models and the values of resonance parameters extracted from data are usually confronted with those coming from constitutive quarks models (QM) and QCD calculations in the lattice. Also, the availability of high intensity ν beams at Fermilab offers a unique opportunity to gain new information on the structure of the nucleon and baryonic resonances. Experiments as MINERνA [5] and FINeSSE [6] will address relevant problems like the extraction of the nucleon and $N \to \Delta$ axial form factors (ANΔ) or the measure of the strange spin of the nucleon.

The weak pion production is closely related to other pion production reactions that involve the Δ resonance. For instance, pion photoproduction $\gamma N \to N'\pi$ and pion electroproduction $eN \to e'N'\pi$ processes have been also extensively studied and have revealed important information on the electromagnetic form factors (FF). From the multipole $\gamma N \to \Delta$ amplitudes $M_{1+}^{3/2}$ and $E_{1+}^{3/2}$ it is possible to extract the values for the transition FF, G_M and G_E, at $q^2 = 0$ (q is the photon momentum) [7–11] using dynamical models. As it is well known, the ratio $R_E = -\operatorname{Im} E_{1^+}^{3/2} / \operatorname{Im} M_{1^+}^{3/2}|_{E_\gamma = M_\Delta}$ is closely related to the size of the nucleon deformation. Also, pion electroproduction brings the possibility to analyze the momentum dependence at $q^2 \neq 0$ of the mentioned FF [12,13].

The weak and electromagnetic currents of some hadrons are closely related to each other via isospin symmetry. Pursuing with the program of describing resonant parameters having at the same time a consistent determination of the pion weak production cross section, it would be important to extend the models previously used in the electromagnetic case to fix the $N \to \Delta$ weak FF (WNΔ). Along the last three decades there have been developed dynamical models studying these FF for the free space cross section. In particular, we mention the contribution of Fogli and Nardulli [14], where the amplitude was calculated at the tree-level by introducing *some* non-resonant terms

* Corresponding author.
E-mail address: mariano@fisica.unlp.edu.ar (A. Mariano).
[1] On sabbatical leave from Departamento de Física, Cinvestav, Apartado Postal 14-740, 07000 México D.F., Mexico.

0370-2693/$ – see front matter
doi:10.1016/j.physletb.2008.05.011

and the Δ resonance through the Rarita–Schwinger (RS) fields. Recently, there has been a renewed interest [15–18] on these topics due to the new neutrino scattering experiments mentioned above, aiming to compare form factors at $q^2 = 0$ values (now q is the momentum transferred by the W bosons) with those obtained from quite recent QCD calculations on the lattice [19] and including nuclear medium effects [20]. Among the main features of these contributions we find: (i) the use of the QM to fix the axial parameters [15]; (ii) they treat the production ($WN \to \Delta$) and decay ($\Delta \to \pi N$) vertexes in an independent way [16]; (iii) they consider the effects of final state interactions (FSI) and meson exchange contributions [17]; (iv) they extend the model of Fogli and Nardulli by including other non-resonant terms and additional FF in the WNΔ vertex [18].

Most of the previous works mentioned above treat inconsistently the vertexes and the propagator of Δ resonance. As mentioned in [21], the Lagrangian densities $\hat{\mathcal{L}}_{\Delta}(A)$ (kinetic term) and $\hat{\mathcal{L}}_{\pi N\Delta}(A)$ (interaction term) are invariant under the contact transformation on the ψ^{μ}_{Δ} field

$$\psi^{\mu}_{\Delta} \to \psi^{\mu}_{\Delta} + a\gamma^{\mu}\gamma_{\alpha}\psi^{\alpha}_{\Delta}, \qquad A \to A' = \frac{A-2a}{1+4a},$$

where A and a ($a \neq -1/4$) are arbitrary parameters. This invariance assures that spurious spin-1/2 components are removed from the field describing an on-shell Δ particle [22]. The Feynman rules involving the propagator and vertexes of the Δ depend on A, but the physical amplitudes are independent of this parameter, as it should be. As shown in Ref. [21] the A-dependent Feynman rules involving the Δ can be replaced by a set of A-independent vertexes and propagators called *reduced* Feynman rules. This scheme was recently extended to include the $\hat{\mathcal{L}}_{\gamma N\Delta}(A)$ Lagrangian looking for the A-independent $\gamma N \to \Delta$ vertex, consistent with the reduced Δ propagator [21]. Since the vector part of the weak $N \to \Delta$ (V$N\Delta$) vertex is related to the electromagnetic vertex $\gamma N\Delta$ through the CVC hypothesis, it is clear that we also need to use a weak production vertex *consistent* with the reduced Δ propagator. Nevertheless, this consistency condition has not been preserved in some of the previous works and we judge important to know how this fact affects the results on the one pion weak production cross section. On the other hand, it has been also shown that FSI between both the final pion and nucleon play an important role in 'dressing' the $\gamma N \to \Delta$ vertex [8,11,12] in such way that the bare $G^0_{M,E}$ values are roughly 40% below the dressed ones. With a lower percentage, this fact has been corroborated in the WNΔ case [17]. Nevertheless, it is common to observe that some works do not consider the influence of FSI [14,18].

In the present Letter we propose an effective Lagrangian model for the calculation of one pion production cross section and the extraction of the ANΔ FF, $F^A_{\Delta}(q^2)$. Our formalism is fully consistent and extends to the weak pion production case the model used to treat elastic and radiative $\pi^+ p$ scattering [23] and pion photoproduction [11]. The N, Δ, π, ρ and ω degrees of freedom and their interactions are introduced by preserving electromagnetic gauge invariance and invariance under contact transformations, when the finite width of the Δ resonance is considered. FSI effects on $F^A_{\Delta}(0)$ are included considering that it is an effective parameter (bare + rescattering contributions) fixed from a fitting procedure to reproduce the experimental data, as we have done previously for the photoproduction case [11].

In this work we analyze as a first step the charged current (CC) modes

$$\nu p \to \mu^- p\pi^+, \qquad \nu n \to \mu^- n\pi^+, \qquad \nu n \to \mu^- p\pi^0, \tag{1}$$

where the tree-level amplitudes are shown schematically in Fig. 1. Clearly, all the Feynman graphs do not necessarily contribute to each of the processes in Eq. (1). We have a non-resonant or background (B) contribution built up of the nucleon Born terms (Fig. 1(a)–(d)), the meson exchange amplitudes (Figs. 1(e) and 1(f)) and the Δ-crossed term (Fig. 1(g)); the genuine resonant contribution (R) coming from the Δ-pole amplitude is shown in Fig. 1(h). The sum of all these terms give rise to the total amplitude which can be separated into a background and a resonant contributions as

$$\mathcal{M} = \mathcal{M}_B + \mathcal{M}_R,$$

where[2]

$$\mathcal{M}_i = -\frac{G_F V_{ud}}{\sqrt{2}}\bar{u}(\mathrm{p}_{\mu})\gamma_{\lambda}(1-\gamma_5)u(\mathrm{p}_{\nu})\bar{u}(\mathrm{p}')\mathcal{O}^{\lambda}_i(\mathrm{p},\mathrm{p}',\mathrm{q})u(\mathrm{p}), \quad i = B, R, \tag{2}$$

with $G_F = 1.16637 \times 10^{-5}$ GeV^{-2}, $|V_{ud}| = 0.9740$, and the 4-momenta defined as

$$\mathrm{p} = (E_N, \mathbf{p}), \qquad \mathrm{p}_{\nu} = (E_{\nu}, \mathbf{p}_{\nu}), \qquad \mathrm{p}_{\mu} = (E_{\mu}, \mathbf{p}_{\mu}), \qquad \mathrm{k} = (E_{\pi}, \mathbf{k}), \qquad \mathrm{p}' = (E_{N'}, \mathbf{p}'),$$

with $E_i = \sqrt{|\mathbf{p}_i|^2 + m_i^2}$ ($|\mathbf{v}_i| = \frac{|\mathbf{p}_i|}{E_i}$ and we set $m_{\nu} = 0$).

It is well known that the baryonic currents J^{λ}_i have a vector-axial structure ($J^{\lambda}_i \equiv V^{\lambda}_i - A^{\lambda}_i$). In terms of the vector current, the electromagnetic one is written as $J^{\lambda}_{\mathrm{elect}} = V^{\lambda}_{\mathrm{isoscalar}} + V^{\lambda}_3$ and the weak CC as $V^{\lambda}_{\pm} \equiv \mp(V^{\lambda}_1 \pm iV^{\lambda}_2)$. The conserved vector current (CVC) hypothesis allows to relate the isovector pieces of these vector currents. In this way, the Born and ω-exchange contributions (ρ-exchange graph (f) do not contribute to V since the $\rho - \pi$ current is isoscalar) can be obtained from the usual strong [23] ($\mathcal{L}_{NN\omega}(x)$ is built from $\mathcal{L}_{NN\rho}(x)$ with the replacements $\rho_{\mu}(x) \to \omega_{\mu}(x)$ and $\boldsymbol{\tau} \to 1$) and electromagnetic interaction Lagrangians [7,11,23]. For the axial currents we adopt the Lagrangians of Refs. [15,17] based on standard effective chiral methods and spin-parity arguments. We get

$$\begin{aligned}
&\mathcal{O}^{\lambda}_B(\mathrm{p},\mathrm{p}',\mathrm{q}) \\
&\quad = -i\sqrt{2}\left[F_1^V(Q^2)\gamma^{\lambda} - i\frac{F_2^V(Q^2)}{2m_N}\sigma^{\lambda\nu}q_{\nu} - F^A(Q^2)\gamma^{\lambda}\gamma_5\right] i\frac{\not{\mathrm{p}}' + \not{\mathrm{q}} + m_N}{(p'+q)^2 - m_N^2}\frac{g_{\pi NN}}{2m_N}\gamma_5(\not{\mathrm{p}} - \not{\mathrm{p}}' - \not{\mathrm{q}})\mathcal{T}_1(m_t m_{t'}) \\
&\qquad + \frac{g_{\pi NN}}{2m_N}\gamma_5(\not{\mathrm{p}} - \not{\mathrm{p}}' - \not{\mathrm{q}}) i\frac{\not{\mathrm{p}} - \not{\mathrm{q}} + m_N}{(p-q)^2 - m_N^2}(-i)\sqrt{2}\left[F_1^V(Q^2)\gamma^{\lambda} - i\frac{F_2^V(Q^2)}{2m_N}\sigma^{\lambda\nu}q_{\nu} - F^A(Q^2)\gamma^{\lambda}\gamma_5\right]\mathcal{T}_2(m_t m_{t'})
\end{aligned}$$

[2] We work in the limit of the local four-fermion interaction.

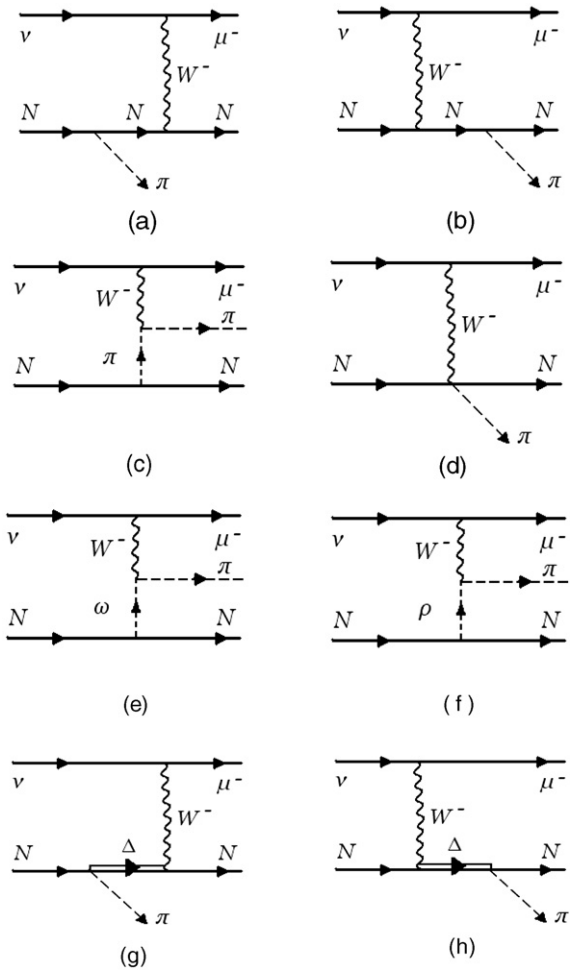

Fig. 1. Contributions to the scattering amplitude for the process $\nu N \to \mu N' \pi$. The Feynman diagrams in (a)–(g) show the 'background' contributions, while the resonant one is shown in (h).

$$
\begin{aligned}
&- i\sqrt{2}F_1^V\left(Q^2\right)(2\mathrm{p}-2\mathrm{p}'-\mathrm{q})^\lambda \frac{i}{(\mathrm{p}-\mathrm{p}')^2-m_\pi^2}\frac{g_{\pi NN}}{2m_N}\gamma_5(\not{\mathrm{p}}-\not{\mathrm{p}}')\mathcal{T}_3(m_t m_{t'}) + \frac{g_{\pi NN}}{2m_N}\sqrt{2}F_1^V\left(Q^2\right)\gamma_5\gamma^\lambda\mathcal{T}_4(m_t m_{t'})\\
&+ i\frac{g_{\omega\pi V}}{m_\omega}\sqrt{2}F_1^V\left(Q^2\right)\epsilon^{\lambda\alpha\beta\delta}\mathrm{q}_\alpha(\mathrm{p}-\mathrm{p}')_\beta i\frac{-g_{\delta\epsilon}}{(\mathrm{p}-\mathrm{p}')^2-m_\omega^2}(-i)\frac{g_{\omega NN}}{2}\left(\gamma^\epsilon - i\frac{\kappa_\omega}{2m_N}\sigma^{\epsilon\kappa}(\mathrm{p}-\mathrm{p}')_\kappa\right)\mathcal{T}_5(m_t m_{t'})\\
&+ f_{\rho\pi A}\sqrt{2}F^A\left(Q^2\right)i\frac{-g^{\lambda\mu}}{(\mathrm{p}-\mathrm{p}')^2-m_\rho^2}(-i)\frac{g_{\rho NN}}{2}\left(\gamma_\mu - i\frac{\kappa_\rho}{2m_N}\sigma_{\mu\kappa}(\mathrm{p}-\mathrm{p}')^\kappa\right)\mathcal{T}_6(m_t m_{t'})\\
&+ \overline{\mathcal{W}^{\lambda\alpha}(-\mathrm{p}_\Delta,\mathrm{q},-\mathrm{p}')}iG_{\alpha\beta}(\mathrm{p}_\Delta=\mathrm{p}'+\mathrm{q})(-)\frac{f_{\pi N\Delta}}{m_\pi}(\mathrm{p}-\mathrm{p}'-\mathrm{q})^\beta\mathcal{T}_7(m_t m_{t'}),
\end{aligned}
\tag{3}
$$

$$
\mathcal{O}_R^\lambda(\mathrm{p},\mathrm{p}',\mathrm{q}) = -\frac{f_{\pi N\Delta}}{m_\pi}(\mathrm{p}-\mathrm{p}'-\mathrm{q})^\alpha iG_{\alpha\beta}(\mathrm{p}_\Delta=\mathrm{p}-\mathrm{q})\mathcal{W}^{\beta\lambda}(p_\Delta,\mathrm{q},\mathrm{p})\mathcal{T}_8(m_t m_{t'}),
\tag{4}
$$

where $q = p_\mu - p_\nu$ is the momentum transferred by leptons and $Q^2 \equiv -q^2$. Here we have defined the isospin matrix elements

$$
\begin{aligned}
\mathcal{T}_1(m_t m_{t'}) &= \chi^\dagger(m_{t'})\left(\boldsymbol{\tau}\cdot\boldsymbol{W}^*\right)\left(\boldsymbol{\tau}\cdot\boldsymbol{\Phi}_\pi^*\right)\chi(m_t)/2,\\
\mathcal{T}_2(m_t m_{t'}) &= \chi^\dagger(m_{t'})\left(\boldsymbol{\tau}\cdot\boldsymbol{\Phi}_\pi^*\right)\left(\boldsymbol{\tau}\cdot\boldsymbol{W}^*\right)\chi(m_t)/2,\\
\mathcal{T}_3(m_t m_{t'}) &= -i\chi^\dagger(m_{t'})\left[\left(\boldsymbol{\Phi}_\pi^*\times\boldsymbol{\Phi}_{\pi'}\right)\cdot\boldsymbol{W}^*\right]\left(\boldsymbol{\tau}\cdot\boldsymbol{\Phi}_{\pi'}^*\right)\chi(m_t),\\
\mathcal{T}_4(m_t m_{t'}) &= i\chi^\dagger(m_{t'})\left[\left(\boldsymbol{\Phi}_\pi^*\times\boldsymbol{\tau}\right)\cdot\boldsymbol{W}^*\right]\chi(m_t),\\
\mathcal{T}_5(m_t m_{t'}) &= \chi^\dagger(m_{t'})\left(\boldsymbol{\Phi}_\pi^*\cdot\boldsymbol{W}^*\right)\chi(m_t),\\
\mathcal{T}_6(m_t m_{t'}) &= i\chi^\dagger(m_{t'})\left[\left(\boldsymbol{\Phi}_\pi^*\times\boldsymbol{\rho}\right)\cdot\boldsymbol{W}^*\right]\left(\boldsymbol{\tau}\cdot\boldsymbol{\rho}^*\right)\chi(m_t),\\
\mathcal{T}_7(m_t m_{t'}) &= \chi^\dagger(m_{t'})\left(\boldsymbol{T}\cdot\boldsymbol{W}^*\right)\left(\boldsymbol{T}^\dagger\cdot\boldsymbol{\Phi}_\pi^*\right)\chi(m_t),\\
\mathcal{T}_8(m_t m_{t'}) &= \chi^\dagger(m_{t'})\left(\boldsymbol{T}\cdot\boldsymbol{\Phi}_\pi^*\right)\left(\boldsymbol{T}^\dagger\cdot\boldsymbol{W}^*\right)\chi(m_t),
\end{aligned}
\tag{5}
$$

with m_t and $m_{t'}$ being the isospin projections of the initial and final state nucleons, respectively, $\boldsymbol{T}^\dagger$ is the $N \to \Delta$ isospin excitation operator, and $\boldsymbol{\Phi}_\pi$, $\boldsymbol{\rho}$ and $\boldsymbol{W}$ are the isospin wave functions of the π and ρ mesons and intermediate boson, respectively. The $N \to B$ weak vector currents ($B = N'$ or Δ) above are obtained from the $\gamma N \to B$ electromagnetic transitions, by assuming CVC hypothesis. In addition to the terms shown in Eq. (3), we include the so-called pion-pole amplitudes (i.e., an intermediate pion is introduced in the W propagation line) through the same procedure discussed in Ref. [17]. The different masses, coupling constants and FF in the above formulas will be given below.

The expression for the *reduced* Δ propagator is given by [21],

$$G_{\alpha\beta}(\mathrm{p}) = \frac{\not{\mathrm{p}} + m_\Delta}{\mathrm{p}^2 - m_\Delta^2}\left\{-g_{\alpha\beta} + \frac{1}{3}\gamma_\alpha\gamma_\beta + \frac{1}{3m_\Delta}(\gamma_\alpha \mathrm{p}_\beta - \gamma_\beta \mathrm{p}_\alpha) + \frac{2}{3m_\Delta^2}\mathrm{p}_\alpha \mathrm{p}_\beta - \frac{2(\mathrm{p}^2 - m_\Delta^2)}{3m_\Delta^2}\left[\gamma_\alpha \mathrm{p}_\beta - \gamma_\beta \mathrm{p}_\alpha - (\not{\mathrm{p}} + m_\Delta)\gamma_\alpha\gamma_\beta\right]\right\}, \tag{6}$$

where the unstable character of the Δ will be introduced by the replacement $m_\Delta \to m_\Delta - i\Gamma_\Delta/2$ [21]. For the $\mathcal{W}^{\beta\lambda}$ vertex we have several equivalents forms, which are consistent with the Δ propagator and strong $\pi N\Delta$ vertex and respect the invariance under contact transformations. The weak interaction Lagrangian $\hat{\mathcal{L}}_{WN\Delta}(A)$ compatible with the free $\hat{\mathcal{L}}_\Delta(A)$ and strong interacting Lagrangian $\hat{\mathcal{L}}_{\pi N\Delta}(A)$ that make possible also a definition of a *reduced* $\mathcal{W}^{\beta\lambda}$ vertex, i.e. A-independent amplitudes, is [11,21]

$$\hat{\mathcal{L}}_{WN\Delta}(x) = i\bar{\psi}_{\Delta\nu}(x)\Lambda^{\nu\nu'}(A)\left(\hat{\mathcal{V}}^V_{\nu'\mu} + \hat{\mathcal{V}}^A_{\nu'\mu}\right)\left(\boldsymbol{T}^\dagger \cdot \boldsymbol{W}\right)\psi_N(x) + \text{h.c.},$$

with

$$\Lambda^{\nu\mu}(A) = g^{\nu\mu} + \frac{1}{2}(1 + 3A)\gamma^\nu\gamma^\mu. \tag{7}$$

The previous Lagrangian leads to the same $\mathcal{W}^V_{\nu\mu}$ vector vertex as in pion photo- [11] and electroproduction [13]

$$\mathcal{W}^V_{\nu\mu}(\mathrm{p}_\Delta, \mathrm{q}, \mathrm{p}) = \sqrt{2}\left[\left(G_M(\mathrm{Q}^2) - G_E(\mathrm{Q}^2)\right)K^M_{\nu\mu} + G_E(\mathrm{Q}^2)K^E_{\nu\mu} + G_C(\mathrm{Q}^2)K^C_{\nu\mu}\right], \tag{8}$$

where $K^M_{\nu\mu}$, $K^E_{\nu\mu}$, and $K^C_{\nu\mu}$ are defined as [24]

$$\begin{aligned}
K^M_{\nu\mu} &= -\frac{3(m_N + m_\Delta)}{2m_N\left((m_N + m_\Delta)^2 + \mathrm{Q}^2\right)}\epsilon_{\nu\mu\alpha\beta}(\mathrm{p} + \mathrm{p}_\Delta)^\alpha \mathrm{q}^\beta,\\
K^E_{\nu\mu} &= \frac{3(m_N + m_\Delta)}{m_N\left((m_N + m_\Delta)^2 + \mathrm{Q}^2\right)\left((m_\Delta - m_N)^2 + \mathrm{Q}^2\right)}\epsilon_{\nu\lambda\alpha\beta}(\mathrm{p} + \mathrm{p}_\Delta)^\alpha \mathrm{q}^\beta \epsilon^\lambda_{\mu\gamma\delta}\mathrm{p}^\gamma_\Delta \mathrm{q}^\delta i\gamma_5,\\
K^C_{\nu\mu} &= \frac{3(m_N + m_\Delta)}{2m_N\left((m_N + m_\Delta)^2 + \mathrm{Q}^2\right)\left((m_\Delta - m_N)^2 + \mathrm{Q}^2\right)}q_\nu\left[\mathrm{Q}^2(\mathrm{p} + \mathrm{p}_\Delta)_\mu + \mathrm{q}\cdot(\mathrm{p} + \mathrm{p}_\Delta)\mathrm{q}_\mu\right]\gamma_5.
\end{aligned} \tag{9}$$

For the axial contribution we use the model given in Refs. [15,17], which is compatible with $\mathcal{W}^V_{\nu\mu}$ (it could be, in principle, obtained by using $-\mathcal{W}^V_{\nu\mu}\gamma_5$) and reads

$$\mathcal{W}^A_{\nu\mu}(\mathrm{p}_\Delta, \mathrm{q}, \mathrm{p}) = -i\left[-D_1(\mathrm{Q}^2)g_{\nu\mu} + \frac{D_2(\mathrm{Q}^2)}{m_N^2}(\mathrm{p} + \mathrm{p}_\Delta)^\alpha(g_{\nu\mu}\mathrm{q}_\alpha - \mathrm{q}_\nu g_{\alpha\mu}) - \frac{D_3(\mathrm{Q}^2)}{m_N^2}\mathrm{p}_\nu \mathrm{q}_\mu + i\frac{D_4(\mathrm{Q}^2)}{m_N^2}\epsilon_{\mu\nu\alpha\beta}(\mathrm{p} + \mathrm{p}_\Delta)^\alpha \mathrm{q}^\beta\gamma_5\right]. \tag{10}$$

The $G_i(\mathrm{Q}^2)$ and $D_i(\mathrm{Q}^2)$ form factors will also be described below. Usually, some authors drop out the second term within square brackets of the Δ propagator from Eq. (6), namely: they use the RS propagator. This procedure introduces inconsistencies since we need the *full* propagator together with the above $\mathcal{W}_{\nu\mu}$ vertexes to get A-independent amplitudes.

Next, we are going to compare our model with experimental data of the total and differential cross sections for weak production of single pions. In terms of the center of mass (CM) variables the total cross section will be calculated from[3]

$$\sigma\left(E_\nu^{\mathrm{CM}}\right) = \frac{m_\mu m_N^2}{(2\pi)^4 E_\nu^{\mathrm{CM}}\sqrt{s}}\int_{E_\mu^-}^{E_\mu^+} dE_\mu^{\mathrm{CM}}\int_{E_\pi^-}^{E_\pi^+} dE_\pi^{\mathrm{CM}}\int_{-1}^{+1} d\cos\theta\int_0^{2\pi} d\eta\,\frac{1}{16}\sum_{\text{spin}}|\mathcal{M}|^2, \tag{11}$$

where $\sqrt{s} = E_\nu^{\mathrm{CM}} + E_N^{\mathrm{CM}}$, the angular variables come from the integration elements $d\Omega_\mu = d\cos\theta\, d\phi$ and $d\Omega_\pi = d\cos\xi\, d\eta$ ($d\phi$ integration gives a factor 2π and $\cos\xi$ is fixed by energy conservation) and

$$\begin{aligned}
E_\mu^- &= m_\mu, \qquad E_\mu^+ = \frac{s + m_\mu^2 - (m_N + m_\pi)^2}{2(E_\nu^{\mathrm{CM}} + E_N^{\mathrm{CM}})},\\
E_\pi^\pm &= \frac{(\sqrt{s} - E_\mu^{\mathrm{CM}})(s - 2\sqrt{s}E_\mu^{\mathrm{CM}} - \Delta^2) \pm A\sqrt{(E_\mu^{\mathrm{CM}})^2 - m_\mu^2}}{2(s - 2\sqrt{s}E_\mu^{\mathrm{CM}} + m_\mu^2)},
\end{aligned} \tag{12}$$

with

$$A = \sqrt{\left(s - 2\sqrt{s}E_\mu^{\mathrm{CM}} - \Delta^2\right)^2 - 4m_\pi^2\left(s - 2\sqrt{s}E_\mu^{\mathrm{CM}} + m_\mu^2\right)}, \quad \Delta^2 = m_N^2 - m_\mu^2 - m_\pi^2. \tag{13}$$

The neutrino CM energy, E_ν^{CM}, is related with the laboratory one as $E_\nu^{\mathrm{CM}} = \frac{m_N E_\nu^{\mathrm{Lab}}}{\sqrt{2E_\nu^{\mathrm{Lab}}m_N + m_N^2}}$.

[3] In order to simplify the calculation we use for the final state particles a frame where the z axis coincides with the muon direction while the y axis is orthogonal to the muon–pion plane; we return to the laboratory frame (where the neutrino is in the z direction) through a rotation.

The differential cross section is computed from

$$\frac{d\sigma}{dQ^2} = \frac{m_\mu m_N^2}{2(2\pi)^4 (E_\nu^{\rm CM})^2 \sqrt{s}} \int_{E_\mu^-}^{E_\mu^+} \frac{dE_\mu^{\rm CM}}{\sqrt{(E_\mu^{\rm CM})^2 - m_\mu^2}} \int_{E_\pi^-}^{E_\pi^+} dE_\pi^{\rm CM} \int_0^{2\pi} d\eta \frac{1}{16} \sum_{\rm spin} |\mathcal{M}|^2, \tag{14}$$

where now $E_\mu^- = (Q^2 + m_\mu^2)/4E_\nu^{\rm CM} + m_\mu^2 E_\nu^{\rm CM}/(Q^2 + m_\mu^2)$ for a fixed value of Q^2. Finally, in order to compare with the experiment, we calculate the neutrino's flux averaged cross section

$$\frac{d\langle\sigma\rangle}{dQ^2} = \int_{E_\nu^{\rm min}}^{E_\nu^{\rm max}} \frac{d\sigma(E_\nu)}{dQ^2} \Phi(E_\nu)\, dE_\nu \Big/ \int_{E_\nu^{\rm min}}^{E_\nu^{\rm max}} \Phi(E_\nu)\, dE_\nu, \tag{15}$$

where $\Phi(E_\nu)$ is the flux of neutrinos corresponding to each experiment.

Now, we give some details about the values of coupling constants and FF used in our calculation. In order to remain consistent, the coupling constants we use in the present work are taken from previous works on pion–nucleon scattering and analysis of photoproduction and electroproduction of pions. For the strong couplings of nucleons we take $g_{\pi NN}^2/4\pi = 14$, $g_{\rho NN}^2/4\pi = 2.9$, $\kappa_\rho = 3.7$, $g_{\omega NN} = 3g_{\rho NN}$ and $\kappa_\omega = -0.12$ [23] with the usually adopted masses for involved hadrons [25]. Note that couplings of nucleons to ρ and ω mesons were obtained by assuming the vector dominance model. For the Δ mass, width and πN coupling constant we assume consistently values obtained previously from the fitting to the $\pi^+ p$ scattering data [11], namely: $f_{N\pi\Delta}^2/4\pi = 0.317 \pm 0.003$, $m_\Delta = 1211.7 \pm 0.4$ MeV and $\Gamma_\Delta = 92.2 \pm 0.4$ MeV.

In the weak sector the vector coupling constants are fixed by assuming the CVC hypothesis both for B and R amplitudes. As usual, for the axial currents we exploit the PCAC hypothesis and the Goldberger–Treiman relations. For the nucleon Born and meson exchange contributions we adopt $g_V = 1$, $g_{\omega\pi V} = g_{\omega\pi\gamma} = 0.3247e$ [11], while for the axial couplings we assume $g_A = 1.26$ (PCAC value) and $f_{\rho\pi A} = \frac{m_\rho^2}{(93\ \text{MeV}) g_{\rho NN}}$ [17]. For the FF we adopt the usual Sachs dipole model for the vector current [14,17] and also a dipole FF for the axial one [17]:

$$\begin{aligned}
F_1^V(Q^2) &= \frac{g_V}{1+t}\left[G_E^p(Q^2) - G_E^n(Q^2) + t\left(G_M^p(Q^2) - G_M^n(Q^2)\right)\right],\\
F_2^V(Q^2) &= \frac{g_V}{1+t}\left[\left(G_M^p(Q^2) - G_M^n(Q^2)\right) - \left(G_E^p(Q^2) - G_E^n(Q^2)\right)\right],\\
F^A(Q^2) &= \frac{g_A}{(1+Q^2/M_A^2)^2}, \qquad M_A = 1.032\ \text{GeV},
\end{aligned} \tag{16}$$

where $t = Q^2/4m_N^2$ and

$$G_E^p(Q^2) = \frac{1}{1+\kappa_p} G_M^p(Q^2) = \frac{1}{\kappa_n} G_M^n(Q^2) = \frac{1}{1+Q^2/M_V^2}, \qquad G_E^n(Q^2) = 0,$$

with $M_V^2 = 0.71$ GeV^2, $\kappa_p = 1.79$ and $\kappa_n = -1.91$. In the case of the contribution involving the $W\pi\pi$ vertex (third term in Eq. (3)) we adopt the same $F_V^1(Q^2)$ as in the other Born terms (first, second and fourth terms in Eq. (3)) since these together should form a gauge invariant amplitude in the electromagnetic case.

For the vector Δ contribution to the B and R amplitudes we use the effective (empirical) values $G_M(0) = 2.97$, $G_E(0) = 0.055$ and $G_C(0) = \frac{2m_\Delta}{m_N - m_\Delta} G_E(0)$ fixed from photo and electroproduction reactions [11,13]. We call these "effective" values, as discussed in Ref. [11], because they correspond to the bare ones $G_i^0(0)$ (usually related with QM) *renormalized* through the decay of a πN state coming from the B amplitude into a Δ (FSI). In Ref. [11] we also get the bare $G_{E,M}^0(0)$ values by introducing dynamically the FSI by an explicit evaluation of the rescattering amplitudes and show that the effective values, which are obtained through a fitting procedure, can be in fact interpreted as the "dressed" ones. For the FF we adopt

$$G_i(Q^2) = G_i(0)\left(1 - Q^2/M_V^2\right)^{-2}\left(1 + aQ^2\right)e^{-bQ^2},$$

with $a = 0.154/(\text{GeV}/c)^2$ and $b = 0.166/(\text{GeV}/c)^2$, for $i = M, E, C$, which corresponds also to a Sachs dipole model times a correction factor already used in electroproduction calculations [13]. The axial FF at $Q^2 = 0$, $F_\Delta^A(0) \equiv D_i(0)$, $i = 1, 4$, are obtained by comparing the non-relativistic limit of $\bar{u}_\Delta^\nu \mathcal{W}_{\nu\mu}^A u$ in the Δ rest frame ($p_\Delta = (m_\Delta, \mathbf{0})$, $p = (E_N(\mathbf{q}), -\mathbf{q})$) with the non-relativistic QM [15,17]. The Q^2 dependence is taken to be the same as in the vector case with a different parameter in the dipole factor, i.e.

$$D_i(Q^2) = D_i(0) F(Q^2), \quad \text{for } i = 1, 2, \qquad D_3(Q^2) = D_3(0) F(Q^2) \frac{m_N^2}{Q^2 + M_\pi^2}, \tag{17}$$

with $M_A = 1.02$ GeV and

$$F(Q^2) = \left(1 + Q^2/M_A^2\right)^{-2}\left(1 + aQ^2\right)e^{-bQ^2}.$$

Here[4]

$$D_1(0) = \frac{6g_A}{5} \frac{m_N + m_\Delta}{2m_N F(-(m_\Delta - m_N)^2)}, \qquad D_2(0) = -D_1(0) \frac{m_N^2}{(m_N + m_\Delta)^2}, \qquad D_3(0) = D_1(0) \frac{2m_N^3}{(m_N + m_\Delta) m_\pi^2}. \tag{18}$$

[4] $F(-(m_\Delta - m_N)^2)$ in the denominator comes from the fact that we scale $D_i(Q^2 = -q^2)$ from the time-like point $q_0^2 = (m_\Delta - m_N)^2$ to $q^2 = 0$ through $F(Q^2)$.

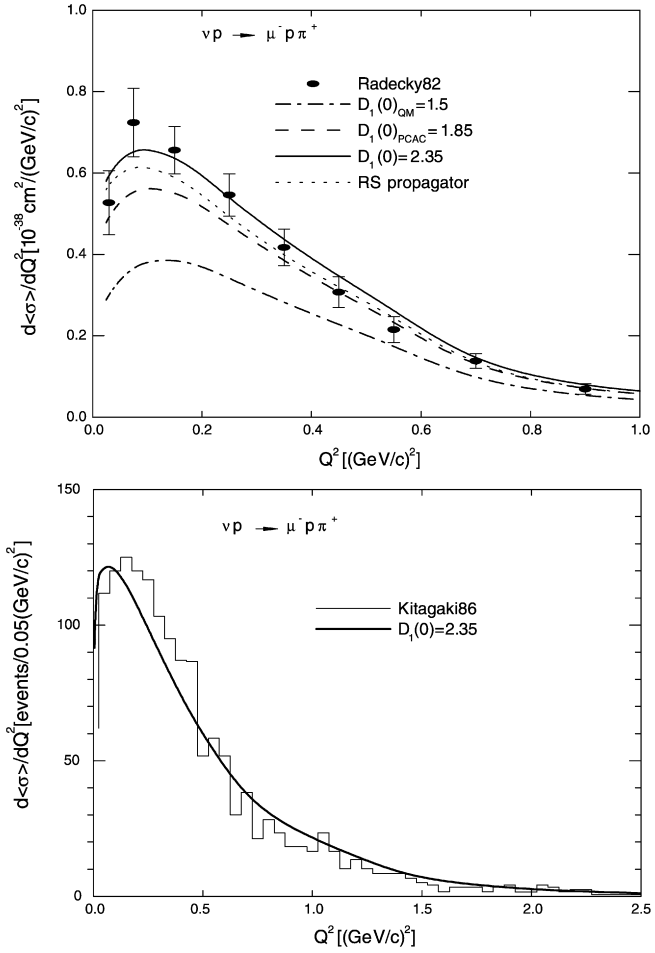

Fig. 2. Comparison of the model and data for the averaged differential cross section of $\nu p \to \mu^- p \pi_+$ scattering as function of Q^2. In the upper panel we show the fitted cross section to the data of Ref. [26], indicated as "Radecki82". In the lower panel we show our predictions for the data of Ref. [28] referred as "Kitagi86".

The last term in Eq. (10) is dropped since we will not take into account the contribution of the Δ deformation to the axial current, i.e., we take $D_4(Q^2) = 0$. Finally, it is important to mention that it is possible to compare the vertex in Eq. (10) with other usual forms in terms of other $C_1^A(Q^2)$, $C_2^A(Q^2), \ldots$ FF (see for example Refs. [14,20]). They related as

$$\frac{D_1(0)}{\sqrt{3}} = C_5^A(0), \qquad \frac{(D_2(0) + D_3(0))}{\sqrt{3}} \approx \frac{D_3(0)}{\sqrt{3}} = C_6^A(0), \qquad \frac{2D_2(0)}{\sqrt{3}} = C_4^A(0).$$

Once we have fixed all the coupling constants for the vector sector of the B and R amplitudes, and the axial ones for the nucleon Born and meson exchange amplitudes, we must decide what is the proper value for the axial FF in the ANΔ vertex. For this purpose we make the calculation of the averaged differential cross section $\frac{d\langle\sigma\rangle}{dQ^2}$ from Eq. (15) for the $\nu p \to \mu^- p \pi^+$ process (the most important process) and the comparison with the ANL experiment in Ref. [26].[5] Since the main dynamical ingredients of the model are the $\Delta(1232)$ resonance and other non-resonant contributions involving nucleons, pions and ρ and ω vector mesons, we will focus in the $m_N + m_\pi \leqslant W \leqslant 1.4$ GeV pion–nucleon invariant mass region, which coincides with the kinematical regions mentioned in the cited experiments. Above this region, higher resonances should be included. The results are shown in the upper panel of Fig. 2. We begin adopting the QM of Eq. (18) $D_1(0) = 1.5$ ($C_5^A(0) = 0.86$), being the corresponding differential cross section shown with dashed-dotted lines. As it can be observed, the corresponding predictions are well below the experimental points, which has been already found in previous calculations using QM FF [15,17]. This fact is not surprising since, as it is well known, FF obtained with the QM are associated with the "bare" values, while are the dressed (by FSI) ones who determine the reaction amplitude to be compared with the experiment.

From our previous work on pion photoproduction [11] we have learn that by dressing the $G_{M,E}(0)$ FF with FSI we reach a good agreement with data. Then, we will also assume here that the value $D_1^0(0) \equiv 1.5$ should be affected by the inclusion of FSI. Another possible choice is to use the PCAC value, $D_1(0) = F_\pi f_{\pi N\Delta}\sqrt{2}/m_\pi = 1.85$, or $C_5^A(0) = 1.07$ (other works usually take the coupling $f^2_{\pi N\Delta}/4\pi = 0.36$ [20] which leads to $C_5^A(0) \simeq 1.2$). Results in this case are shown with dashed lines; as we can observe, theoretical results are still below the experimental cross section. Then, as in the case of pion photoproduction [11], we will consider $D_1(0)$ as a free (effective or empirical) parameter to be fitted from the experimental data for $\frac{d\langle\sigma\rangle}{dQ^2}$ and including the FSI effects. From this fit we get $D_1(0) = 2.35$ ($C_5^A(0) = 1.35$) with $\chi^2/\text{dof} = 0.71$, and results are shown with full lines. The PCAC prediction for this axial parameter lies $\sim 21\%$ below the fitted value

[5] Data from this experiment have been also used recently in Ref. [18].

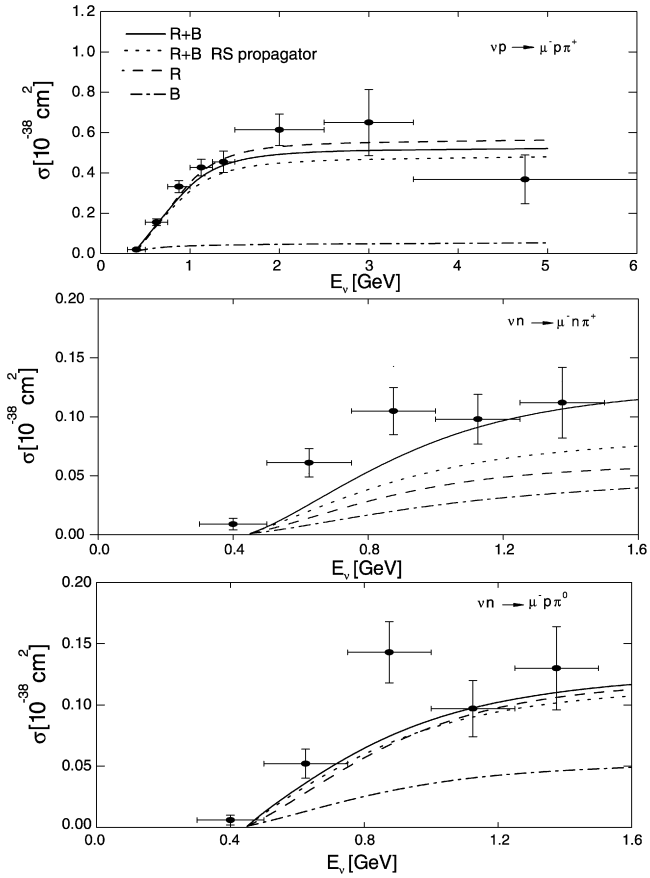

Fig. 3. Comparison of model predictions for the total cross sections of the different $\nu N \to \mu^- N'\pi$ scattering processes.

while the QM underestimates it in $\sim 37\%$. It is important to note that this result is fully consistent with Ref. [15], where for the empirical value they get $D_1(0) = 2.4$, and with Ref. [17], where at $Q^2 = 0$ the QM prediction is 35 % below the empirical WNΔ FF. Quite recent QM determinations ($C_5^A(0) = 0.93$) [27] are also below the empirical values. Another signal of consistence of our results is that in the vector sector $G_M^0(0)$ is strongly affected by FSI obtaining an effective value such that $G_M(0) = 1.7 \times G_M^0(0)$, as shown in our previous work on photoproduction using the same model (see Ref. [11]). Then, we must conclude that, as before for the vector case, the enlargement in the value of the empirical WNΔ FF as regards its corresponding QM value is due to the effect of FSI, which are taken into account at less effectively in the adjustment of $D_1(0)$.

We also display with dotted lines results for the differential cross section by using $D_1(0) = 2.35$, and the RS propagator (obtained by dropping the second term in the Δ propagator from Eq. (6), as done in Refs. [14,17,18]). As we have discussed above, this procedure is inconsistent because the physical amplitudes do not respect invariance under contact transformations. Clearly, the effect of using this truncated propagator is more important at lower values of Q^2. Additionally, in the lower panel of Fig. 2 we compare our prediction for $\frac{d\langle\sigma\rangle}{dQ^2}$ with $D_1(0) = 2.35$ and the full Δ propagator, with the more recent data from the BNL experiment of Ref. [28] (for comparison, we have adopted in this calculation the same neutrino flux as in this reference). Since this data is given in arbitrary units, we normalize the area under our curve to that under the experiment data. We get a reasonable prediction which is consistent with the fitting achieved previously to the ANL data, which indicates that if we would change the data set in the fitting we should not expect very different results.

Next, we evaluate the total cross section (11) for all the three neutrino scattering processes described in Eq. (1) and compare them with the experimental results coming from Ref. [26]. Our results are shown in Fig. 3. There we present separately the plots obtained with the complete Δ propagator for the background (B), resonant (R) and total (B + R) contributions. For completeness, we compare with those achieved with the RS propagator (B + R RS propagator). As it can be observed, we obtain an overall acceptable agreement (considering the size of the error bars) with the experimental cross sections for the three processes. The destructive interference between the B and R amplitudes, already found in previous works [14], is clearly seen. Again, the effect of replacing the full propagator by the RS one is remarkable, especially for the $\nu n \to \mu^- n\pi^+$ process. This happens because in this case B and R are comparable, and we only get an acceptable result when we use the full propagator. Note that in previous works where the RS propagator is used [14,18] the mentioned process is poorly reproduced.

In summary, we have used a consistent dynamical model for weak pion production. Our model is an extension of the ones previously used to describe pion–nucleon scattering and pion photoproduction in a satisfactory way. This is achieved by using simultaneously the form of the Δ propagator which is consistent with the $N \to \Delta$ weak vertex. We have reproduced the data on the total and differential cross sections by adjusting only one parameter, the axial form factor $D_1(0)$ at $Q^2 = 0$, and we have included effectively the FSI. This procedure lead to conclusions on the ANΔ FF in full consistence with previous more evolved models where FSI are introduced dynamically [17] and with QM [15,27]. It would certainly be interesting to analyze the antineutrinos scattering cross sections in the framework of our model because theoretical models and experimental results [29] still exhibit discrepancies and it will be the subject of a future work. In addition,

we have not discussed the neutral current production with our model since the more recent data reanalysis [30] provides the absolute cross section *without* cuts in the pion–nucleon invariant mass W. For a realistic description with $W > 1.4$ GeV we should include more energetic resonances than the $\Delta(1232)$ MeV, absents in the present model, and this issue also will be analyzed in the future.

Acknowledgements

C.B. and A.M. are fellows of the CONICET (Argentina) and acknowledge support under Grant No. PIP 06-6159. G.L.C. acknowledges financial support from Conacyt (Mexico).

References

[1] M. Honda, T. Kajita, K. Kasahara, S. Midorikawa, Phys. Rev. D 52 (1995) 4985.
[2] F. Vissani, A.Yu. Smirnov, Phys. Lett. B 432 (1998) 376.
[3] S. Nakayama, Phys. Lett. B 619 (2005) 255.
[4] J.L. Raaf, Nucl. Phys. B (Proc. Suppl.) 139 (2005) 47.
[5] R. Gran, hep-ex/07113029.
[6] S. Brice, et al., Nucl. Phys. B 139 (2005) 317.
[7] S. Nozawa, T.-S.H. Lee, Nucl. Phys. A 513 (1990) 511.
[8] T. Sato, T.-S.H. Lee, Phys. Rev. C 54 (1996) 2660.
[9] D. Drechsel, O. Hastein, S.S. Kamalov, L. Tiator, Nucl. Phys. A 645 (1999) 145.
[10] C. Fernández-Ramírez, E. Moya de Guerra, J.M. Udías, Ann. Phys. (N.Y.) 321 (2006) 1408.
[11] A. Mariano, Phys. Lett. B 647 (2007) 253;
A. Mariano, J. Phys. G 34 (2007) 1627.
[12] S.S. Kamalov, S.N. Yang, Phys. Rev. Lett. 83 (1999) 4494.
[13] T. Sato, T.-S.H. Lee, Phys. Rev. C 63 (2001) 055201.
[14] G.L. Fogli, G. Nardulli, Nucl. Phys. B 160 (1979) 116.
[15] T.R. Hemmert, B.R. Holstein, Phys. Rev. D 51 (1995) 158.
[16] L. Alvarez-Ruso, S.K. Singh, M.J. Vicente Vacas, Phys. Rev. C 59 (1998) 3386.
[17] T. Sato, D. Uno, T.-S.H. Lee, Phys. Rev. C 67 (2003) 065201.
[18] E. Hernandez, J. Nieves, M. Valverde, Phys. Rev. D 76 (2007) 033005.
[19] C. Alexandrou, Th. Lentiou, J.W. Negele, A. Tsapalis, Phys. Rev. Lett. 98 (2007) 052003.
[20] T. Leitner, L. Alvarez-Ruso, U. Mosel, Phys. Rev. C 73 (2006) 065502.
[21] M. El-Amiri, G. López Castro, J. Pestieau, Nucl. Phys. A 543 (1992) 673.
[22] K. Johnson, E.C.G. Sudarshan, Ann. Phys. 13 (1961) 126.
[23] G. López Castro, A. Mariano, Nucl. Phys. A 697 (2001) 440.
[24] H.F. Jones, M.D. Scadron, Ann. Phys. 81 (1973) 1.
[25] W.-M. Yao, et al., J. Phys. G 33 (2006) 1.
[26] G.M. Radecky, et al., Phys. Rev. D 25 (1982) 1161.
[27] D. Barquilla-Cano, A.J. Buchmann, E. Hernández, Phys. Rev. C 75 (2007) 065203.
[28] T. Kitagi, et al., Phys. Rev. D 34 (1986) 2554.
[29] M. Sajjad Athar, S. Ahmad, K. Singh, Phys. Rev. D 75 (2007) 093003.
[30] E.A. Hawker, in: Proceedings of the Second International Workshop on Neutrino–Nucleus Interactions in The Few GeV Region, Irvine, California, 2002, http://www.ps.uci.edu/nuint/proceedings/hawker.pdf.